Ojo *et al. Beni-Suef Univ J Basic Appl Sci* (2022) 11:82
https://doi.org/10.1186/s43088-022-00262-8

Beni-Suef University Journal of Basic and Applied Sciences

RESEARCH

Open Access

Development and characterization of mupirocin encapsulated in animal bone-derived hydroxyapatite for management of chronic wounds

Olusola Emmanuel Ojo[1,2*], Margaret Okonawan Ilomuanya[3], Olatunde Israel Sekunowo[1], Oluwashina Philips Gbenebor[1] and Samson Oluropo Adeosun[1,4]

Abstract

Background: Hydroxyapatite is an important biomedical material used in drug delivery owing to its excellent bioactivity and biocompatibility. In this study, hydroxyapatite isolated from bovine and caprine bones was capped and used as a drug carrier to encapsulate mupirocin as an active pharmaceutical product in hydrogel formulations which were utilized in wound healing application using animal model (Wistar Rats).

Results: Characterization of the mupirocin-encapsulated hydroxyapatite using Fourier transform infrared spectroscopy, and X-ray diffractometer revealed the active presence of mupirocin after encapsulation. The in-vitro drug release study revealed that the capped hydroxyapatite obtained from caprine bone loaded with mupirocin gave drug release rate of 84.67% of the drug within 75 min while conventional mupirocin ointment had the lowest at 27.04% within the same time. The capped hydroxyapatite obtained from bovine bone loaded with mupirocin had the highest encapsulation efficiency of 73.67%. However, the animals treated with formulation prepared from capped hydroxyapatite obtained from caprine bone loaded with mupirocin had the highest wound closure area of 377.8 mm^2, while conventional mupirocin ointment had 231.5 mm^2 in 16 days of treatment. All the formulations with mupirocin except the ointment showed excellent resistance against *Klebsiella pneumonia* and *Staphylococcus aureus* of about 40 mm of inhibition zone.

Conclusions: The mupirocin encapsulated in hydroxyapatite extracted from bovine and caprine bones has been demonstrated to be more superior to the conventional ointment in the management of chronic wound conditions.

Keywords: Hydroxyapatite, Chronic wound, Mupirocin, Bovine bone, Caprine bone

1 Background

Microparticles and nanoparticles have been progressively studied to achieve targeted and sustained drug release [1]. However, several particles investigated were discovered to be detrimental to human health and the environment during usage and production. For instance, permanent bluish-gray discoloration of the skin (*argyria*) or the eyes (*argyrosis*) is experienced when silver nanoparticles are used for drug delivery in human beings [2]. Zinc oxide nanoparticles are cytotoxic to human cells [3]. Hence, it is imperative to tackle the unmanageable side effects by carefully selecting a drug carrier like Hydroxyapatite (HAP) that is devoid of the side effects. The HAP ($Ca_{10}(PO_4)_6(OH)_2$) is a bio-ceramic material which is a naturally occurring phase of calcium phosphate. It

*Correspondence: isolyet@yahoo.com

[1] Department of Metallurgical and Materials Engineering, Faculty of Engineering, University of Lagos, Akoka, Lagos, Nigeria
Full list of author information is available at the end of the article

Springer Open

© The Author(s) 2022. **Open Access** This article is licensed under a Creative Commons Attribution 4.0 International License, which permits use, sharing, adaptation, distribution and reproduction in any medium or format, as long as you give appropriate credit to the original author(s) and the source, provide a link to the Creative Commons licence, and indicate if changes were made. The images or other third party material in this article are included in the article's Creative Commons licence, unless indicated otherwise in a credit line to the material. If material is not included in the article's Creative Commons licence and your intended use is not permitted by statutory regulation or exceeds the permitted use, you will need to obtain permission directly from the copyright holder. To view a copy of this licence, visit http://creativecommons.org/licenses/by/4.0/.

also exists in other phases like α-Tricalcium Phosphate (α-$Ca_3(PO_4)_2$), β-Tricalcium Phosphate (β-$Ca_3(PO_4)_2$), Tetracalcium Phosphate, etc. The HAP is the most excellent of all the CaP phases, as a result of its outstanding properties like bioactivity, biocompatibility, non-toxicity, non-inflammatory nature, etc. It comprises of about 50% by weight of the bone and its chemical and mineral phases are closely related to bones and teeth [4–7]. The uses of HAP in biomedical field cannot be overemphasized. These vary from bone substitutes, body implants, drug delivery [8] for wound healing. Wound is a physically or thermally induced injury that results in laceration or rupture of the skin epithelial integrity [9]. Wound healing, as a normal, natural, and spontaneous biological process in the human body, can be held up by factors like diabetes, oxidative stress, and infections. For a wound to heal successfully, all the four wound healing phases must take place in the proper sequence and time frame. Hemostasis, which is the first phase that closes the wound by clotting; inflammation, the second phase comes up as primary defense against infections; proliferation phase is characterized by development of new tissues, and remodeling, which is the last brings about the formation of type I collagen and final wound closure [10, 11].

Generally, wounds can be categorized into two namely acute and chronic wounds. The former mainly result from mechanical, thermal damage, high heat exposure, or corrosive chemicals. It takes relatively short period of time for them to heal up if aided by appropriate wound management [12]. The latter fail to progress through the normal stages of healing in a timely manner and usually remain unhealed after 3 months and become stuck in a state of pathologic inflammation [11, 13]. Often, the normal skin has a slightly acidic pH within the range of 4.0–6.3, while chronic wounds generally have an alkaline pH, ranging from 7.15 to 8.93. Wounds with an alkaline pH have shown retarded rates of healing, while an acidic wound bed is an additional benefit that can hasten the wound toward healing [14]. The barrier and skin integrity loss to skin wounds elicit the exposure of open wounds to bacterial colonization and multiplication [15].

There is a loss of balance between collagen production and degradation in chronic wounds; there is more of degradation [16, 17]. The fluid from chronic wounds has an excess of proteases and reactive oxygen species; the fluid itself can slow down healing process by inhibiting cell growth, destroying the proteins and growth factors in the extracellular matrix [18]. When the bioactive molecules are incorporated in the drug carriers, they are protected from degradation prompted by proteases in the wounds, consequently enhancing their therapeutic effectiveness [19]. In the present study, mupirocin (MUP) was encapsulated in HAP derived from bovine and caprine in topical gel, then used for the management of chronic wounds and its wound healing ability was investigated. The MUP normally produced via *Pseudomonas fluorescens* is a potent topical antibiotic agent mainly used for treatment of primary and secondary skin infections by inhibiting the bacterial protein synthesis. It has in vitro activity against a range of gram-positive and some gram-negative bacteria. The body system converts it to monic acid, which is excreted in the urine. It hinders the reproduction and growth of bacteria (bacteriostatic) at lower concentrations, but kill the bacteria (bactericidal) with prolonged exposure, killing up to 99% of susceptible bacteria over a 24 h period [20, 21]. The HAP obtained from bovine and caprine bones through calcination process, capped with moringa seed extract was used to produced MUP-HAP hydrogel composite formulations and were comparatively used alongside conventional MUP ointment in management of chronic wound. The chronic wound condition was simulated by injecting the animal used (Wistar Rats) with alloxan monohydrate.

2 Methods

2.1 Materials

Bovine and caprine femur bones used in this study were purchased at the Magboro central market in Ogun State, Nigeria. The bones were obtained from approximately 36 months old animals. The other materials used are as follows: MUP powder used as the active pharmaceutical ingredient (API) (CAS number 12650-69-0 Shaanxi Top Pharmaceutical Chemical Co. Limited, Shaanxi, China), Conventional MUP ointment (MUP/O) (Mupiderm) (Yash Medicare Pvt Ltd., Gujarat, India), Mueller- Hilton Agar (HiMedia Laboratory Pvt. Limited, India), Carbopol 940 (Hubei New Desheng Materials Technology Co., Ltd, Ezhou city, Hubei province, China), Transcutol P® (Gattefosse Sas Saint-Priest Cedex- France), Moringa seed extract used as the source of oleic acid, Alloxan monohydrate (98% purity, Sigma-Aldrich, USA), Acetic Acid (99.8% purity Sigma-Aldrich, Germany), Methyl paraben, propyl paraben (VA-SUDHA Chemicals PVT LTD, India). All other chemical reagents and solvents used in this study were of analytical grade and were utilized without further purification.

2.2 Bone preparation and calcination

The calcination process was done to remove the organic matters present in the bovine bone sample (BBS) and caprine bone sample (CBS). The defatted and dried BBS and CBS were charged into an electric furnace (Carbonite, England) for calcination at 1000 °C for 2 h. This calcination temperature had been determined by Ojo et al. [22] to be appropriate for formation of high-quality HAP. The samples were allowed to cool to ambient temperature

before removing them from the furnace after which they were hammer-milled and then ball-milled. Before characterization, they were sifted using sieve with 150 µm mesh. The raw BBS and CBS were equally milled, and their particle sizes were determined alongside the calcined samples using Image J® software.

2.3 Moringa seed oil extraction

The moringa seeds (MOS) were thoroughly washed, dried, and divided into two; the first part was processed by milling in a 250 W Panasonic kitchen milling machine model MX-GX1521, two weeks after harvest. A hundred gram (100 g) was weighed and cold pressed. Twelve weeks after harvest, the second portion was milled, pressed, and the leftover was weighed and recorded. This was repeated five times. The oil yield (x) is calculated using Eq. 1.

$$x = \left[\frac{W_b - W_a}{W_b}\right] * 100 \quad (1)$$

where

W_a is the weight after pressing.

W_b is weight before pressing.

2.4 Wound healing formulation

2.4.1 Capping of natural HAP particles

Ten grams each of HAP derived from bovine bone (BHAP) and HAP derived from caprine bone (CHAP) were dispensed into a beaker containing 100 mL of distilled water. Then, 3 mL of MOS was added to the BHAP and CHAP as the source of oleic acid used as natural capping agent. Magnetic stirrer was used for an hour at 1000 rpm for thorough stirring. A hundred milliliters (100 mL) of ethanol was added to each of the solutions, stirred for 5 min then filtered off to remove the MOS. This process was repeated five times. At temperature of 75 °C, the capped BHAP and CHAP were dried in an oven for 24 h, then crushed in a laboratory porcelain mortar and pestle.

2.4.2 Drug loading of BHAP particles

A hundred milliliters (100 mL) of ethanol were dispensed into two beakers and 4 g of MUP was added to each of them, 10 g each of capped BHAP and CHAP were dispersed into the beakers with MUP-ethanol solution. They were stirred at 1000 rpm for 15 min using a magnetic stirrer then centrifuged at 4000 rpm for 5 min. It was dried without heat to avoid the MUP being crystallized. Two milliliters of the supernatant was taken for ultraviolet–visible spectroscopy (UV–VIS) analysis to determine the quantity of free MUP in the ethanol. The encapsulation efficiency (EE) and drug loading capacity (DLC) of the capped BHAP and CHAP were evaluated based on this.

2.4.3 Hydrogel formulations

Five hundred milligrams (0.5 g) of Carbopol 940 was poured into four beakers each with 50 mL of distilled water. The contents were stirred in the beakers and allowed to swell for one hour. Triethanolamine was added and stirred to thicken it and take the pH to about 5.5. Small quantity of propyl paraben (0.01 g) and methyl paraben (0.02 g) as preservatives; 20 mL of propylene glycol as a humectant for the wound hydration were also added. Predetermined volume (0.6 mL) of Transcutol P® was introduced as a penetration enhancer. The formulations were thoroughly stirred for homogeneity and viscosity test was carried out at 20 rpm immediately and after repeated 3 months. The results are shown in Table 1.

2.4.4 Formulation of MUP-HAP hydrogel composite

Five grams (5 g) each of MUP-loaded-capped BHAP (BMM) and CHAP (CMM) was dispensed into each of the previously formulated hydrogel to produce 2%w/v MUP formulations, which is the standard concentration of MUP in conventional topical dosage form. They were made up to 100 mL with distilled water; a spatula was used for thorough stirring to have homogeneity. The formulations' matrices are shown in Table 2.

2.5 Chemical characteristics

2.5.1 Identification of functional groups

The functional groups in the BHAP, CHAP, BMM and CMM were determined with Fourier transform infrared spectroscopy (FTIR) Agilent Technologies® (USA) FTIR analyzer in the range of 4000–650 cm^{-1}. The samples were dehydrated by vacuum drying at 45 °C and positioned over the diamond crystal for the FTIR analysis. Twenty scans were recorded for each spectrum.

Table 1 Viscosity of the formulations

Formulation code	Viscosity (Mpa)	Viscosity after 3 months
BBM	2500 ± 28	2451 ± 26
CMM	2497 ± 25	2446 ± 23
BHAP	2602 ± 23	2563 ± 25
MUP/O	4500 ± 28	–

Table 2 Formulations' matrices

Formulations	MUP (%w/v)	HAP (%w/v)	Transcutol (%v/v)	Carbopol (%w/v)	Propyl paraben (%w/v)	Methyl paraben (%w/v)	Propelene glycol (%v/v)
HAP	------	10	0.6	0.5	0.01	0.02	20
MUP/O	Conventional mupirocin ointment						
BMM	2	10	0.6	0.5	0.01	0.02	20
CMM	2	10	0.6	0.5	0.01	0.02	20

2.5.2 Crystallographic analysis of the samples

The crystal structures of the samples were analyzed on an EMPYERN XRD-600 Diffractometer (45 kV, 40 mA) with a CuKα ($\lambda = 1.54$). Radiation over the scanning range (2θ) is from 5° to 80° and a step size is of 0.026°.

2.6 Determination of encapsulation efficiency and drug loading capacity

The UV–VIS analysis revealed the unencapsulated MUP present in the ethanol after the capped BHAP and CHAP were loaded with drug. Eqs. 2 and 3 are used to determine the percentage of drug that successfully entrapped into the particles (EE), and the quantity of drug that 1 g of the capped BHAP and CHAP particles can encapsulate (DLC), respectively [23].

$$\mathrm{EE} = \left[\frac{\alpha - \beta}{\alpha}\right] * 100 \tag{2}$$

$$\mathrm{DLC} = \frac{\gamma}{\rho} \tag{3}$$

where

α is the Total Drug Loaded.

β is Unencapsulated Drug.

γ is the Total Encapsulated Drug.

ρ is the Total Weight of capped BHAP or CHAP Particles.

2.7 Biological characteristics

2.7.1 In vitro drug release study

The release study of MUP from the BMM and CMM Hydrogel scaffolds alongside MUP/O were modified in situ glass vial system, a 2.5 mL part of each of the formulations was immersed into 50 mL of phosphate- buffered saline (PBS) (pH 7.4). The samples were incubated at 37 ± 0.5 °C and stirred at 100 rpm with a magnetic stirrer. Aliquot of each sample (1 mL) was withdrawn from the release medium at fixed intervals (0, 5, 15, 30, 60 and 75 min) and the same amount of fresh solution was added back to the release medium to maintain sink conditions. Analysis was carried out on the samples using an UV spectrophotometer at 250 nm [24]. Based on the in vitro drug release studies results obtained, the graphs of cumulative percentage of MUP released against time; log cumulative percentage of MUP remaining against time; cumulative percentage of MUP released against square root of time in hour [25] and log cumulative percentage of MUP released against log time in hour [26] were plotted to determine the most suitable kinetic release models, that is, zero order, first order, Higuchi and Korsmeyer-Peppas models, respectively, and the possible release mechanism of the formulations [27].

2.7.2 Evaluation of antibacterial activities

The evaluation of antimicrobial activities of MUP/O, BMM, CMM, BHAP, CHAP and MUPP (Pure MUP powder) were estimated against *Staphylococcus aureus, Staphylococcus saprophyticus, Escherichia coli, and Klebsiella pneumonia* by disk diffusion method using Mueller–Hinton Agar as the medium. As recommended, 38 g of the Agar was dissolved in 1000 mL of distilled water, poured in a bottle and autoclaved for 45 min for sterilization. A volume of 20 mL was poured into each of the four sterile petri dishes (one for each bacterium) in the laminar flow cupboard and the bacteria were introduced to the Agar using sterile swab sticks near a flaming burner to avoid any form of contamination. Paper disks of 6 mm diameter were put on the agar in each of the petri dishes. Normal saline was used for dissolution of MUP, while acetic acid (AA) was used for MUP/O, BMM, CMM, BHAP and CHAP. Ten microliters (10 µL) solution of each sample was introduced to each of the paper disks. They were incubated for 24 h at 37 °C [28], and a metric ruler was used to measure the zones of inhibition in triplicate [29].

2.7.3 In-vivo wound healing study and histology

Thirty (30) male Wistar rats of age 16 weeks were supplied by Priceless Pet Animals, Badagry, Lagos, Nigeria with weight ranging from 140 to 196 g. They were housed at temperature of 28 ± 2 °C and relative humidity of 75 ± 10%. Each of the rats was kept in a semi-transparent polymer cage of dimension 50 × 36 × 23 cm with 23 × 34 cm netted opening on top for good ventilation. They were allowed to

acclimatize for 10 days before the commencement of the experiment. All the guidelines approved by University of Lagos College of Medicine's Health Research Ethical Committee (CMUL/ HREC/03/21/829) were followed during the experiments. Alloxan monohydrate solution at dosage of 150 mg/kg and concentration of 50 mg/ml saline water were prepared to induce Diabetics I in the animals. Their blood sugar was determined with Accu-Check® and recorded before and after 48 h of induction [30]. The wound incisions were made on the dorsum (back of the body) of the rats. Methylated spirit was used to clean the wounds, while digital vernier caliper was utilized to measure the length and width of the wounds using greatest length and width method; the values were recorded to calculate the wound area. One milliliter (1 mL equivalent to 1.16 ± 0.02 g) of BMM, CMM, BHAP hydrogel formulations alongside MUP/O was applied on the wounds of the diabetic animals for 16 days at 2 days interval and then dressed with gauze and plaster. Apart from cleaning and dressing, no formulations were applied on the control rats.

The rats were compassionately euthanized after the 16-day wound treatment period. The incised wound area of each rat was trimmed to include the dermis and the hypodermis and kept in sample bottles filled with 10% neutral buffered formalin to preserve the tissues. After paraffin embedding, 3–4 µm sections were prepared. Representative sections were then stained with hematoxylin and eosin (H&E). Light microscopic examination for histological profiles was performed on individual rat skin sections [24].

3 Results

3.1 Bone calcination

Table 3 shows the percentage weight loss of the BBS and CBS after calcination at 1000 °C. This is the parameter that reveals the quantity of the organic moiety (collagen) that was ejected out of the bone samples. The BBS and CBS had 37% and 45.4% percentage weight loss, respectively. The morphology of raw BBS and CBS look like mass of aggregates that have low surface area and show a wide range of particle size and shapes with edges and corners as shown in Fig. 1. In contrast, the calcined BBS and CBS showed spherical shapes which is the alteration of the raw samples exhibiting higher surface area with average particle size of 8.3 µm and 7.17 µm, respectively.

3.2 Determination MOS extraction yield

Generally, every seed contains 34–45% of oil by weight. The moringa seed contains 36.7% and total extraction is only possible using *n*-hexane, whereas only 69% on average is possible by cold pressing [31]. During cold pressing, the seeds kept for two and twelve weeks after harvest gave oil yield of 3.0% and 19.6%, respectively.

3.3 Chemical characteristics

3.3.1 Identification of functional groups

Fourier transform infrared spectroscopy (FTIR) spectra of the BMM and CMM samples were analyzed and compared with that of BHAP and CHAP as shown in Fig. 2A, B. Both the BHAP and CHAP showed the characteristic bands of HAP. The main peak of phosphate (PO_4^{3-}) (v3) in BHAP and CHAP is at band 1032 and 1021 cm^{-1}, respectively; but there was drastic reduction in their peak intensities after drug loading from 7.2 to 56% in BMM and 7.2 to 46% transmittance in CHAP. The bands of MUP at 2855–2851, 2922–2929 cm^{-1} and oleic acid at 2922–2929 and 2851–2855 cm^{-1} were identified in BMM and CMM.

3.3.2 Crystallographic analysis of BMM, CMM, BHAP and CHAP

The crystallographic analysis was performed on BMM, CMM, BHAP and CHAP. Figure 2C, D show their diffraction patterns. The BHAP and CHAP show the characteristic peaks of a typical HAP. There were some peaks in the diffraction patterns of BMM and CMM that did not appear in the BHAP and CHAP, respectively. They mainly appeared at $2\theta = \sim 6^{\circ}$ and 24° after the drug loading.

3.4 Determination of encapsulation efficiency and drug loading capacity

The UV–VIS analysis revealed that out of 4 g (α) of the MUP loaded to be encapsulated by capped BHAP and CHAP, 1.0540 and 1.1373 g of MUP as shown in Table 4 were found in the 100 mL of the ethanol, respectively. This implied that the mass of MUP that was encapsulated by capped BHAP and CHAP was 2.9460 and 2.8627 g (γ), respectively. Equations 2 and 3 were used to determine the EE and DLC and found to be 73.65% and 295 mg/g,

Table 3 Percentage weight loss of BBS and CBS after calcination

Temp (°C)	Initial weight (g)		Post calcination weight (g)		Weight loss (g)		% Weight loss	
	Bovine	Caprine	Bovine	Caprine	Bovine	Caprine	Bovine	Caprine
1000	500	500	315	273	185	227	37.0	45.4

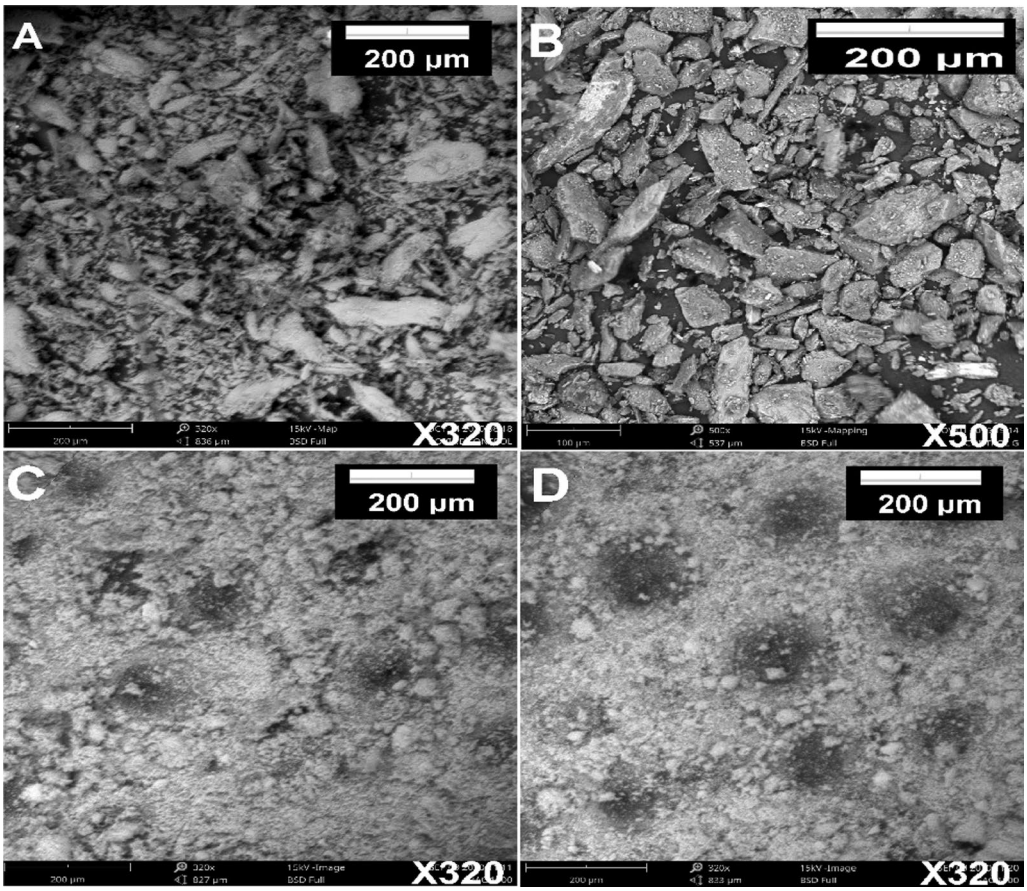

Fig. 1 The scanning electron micrographs of **A** Raw BBS; **B** Raw CBS; **C** Calcined BBS and **D** Calcined CBS at 1000 °C

also 71.57% and 286 mg/g in capped BHAP and CHAP, respectively.

3.4.1 In vitro drug release study

The CMM had the highest drug release rate of 84.67% after 75 min while BMM and MUP/O had 77% and 27.04%, respectively (Fig. 3). The best fitted kinetic release model was determined based on the closeness coefficient of determination (R^2) value to 1 [27]. The highest (R^2) values for formulations CMM and BMM were obtained from Higuchi kinetics and were found to be 0.9921 and 0.9911, respectively, while that of MUP/O was obtained from zero-order kinetics 0.9739 as shown in Fig. 4 and Table 5.

3.4.2 Evaluation of antibacterial activities

The MUP as a topical antibiotic agent from *Pseudomonas fluorescence* has in vitro activities against a range of bacteria [20]. Its presence in BMM, CMM, MUP/O and MUPP (Pure Mupirocin Powder) made them exhibit an excellent activity against the bacteria while the BHAP, CHAP and AA (used for dissolution) did not show any inhibition zone against any of the bacteria used in this study. The BBM, CMM, MUP/O and MUPP all had MUP as the API in them thereby creating high inhibition zone of about 40 mm against the *Klebsiella pneumonia* and *Staphylococcus aureus* except for MUP/O, which had 32.67 mm against *Staphylococcus aureus.* Microbial plates showing evaluation of antibacterial activity of the formulations and the graphical representation of inhibition of zones against the bacteria is shown in Fig. 5. The zone of inhibition was relatively lower against *Staphylococcus saprophyticus* and *Escherichia coli* in all formulations as shown in Fig. 5J. The MUPP had the highest zone of inhibition of 30.66 and 25.55 mm against *Staphylococcus saprophyticus* and *Escherichia coli,* respectively. This is followed by BMM and CMM, MUP/O had the least of 8.83 and 10.33 mm against *Staphylococcus saprophyticus* and *Escherichia coli*, respectively. It was observed that the MUPP had the overall highest inhibition zone against each of the four bacteria.

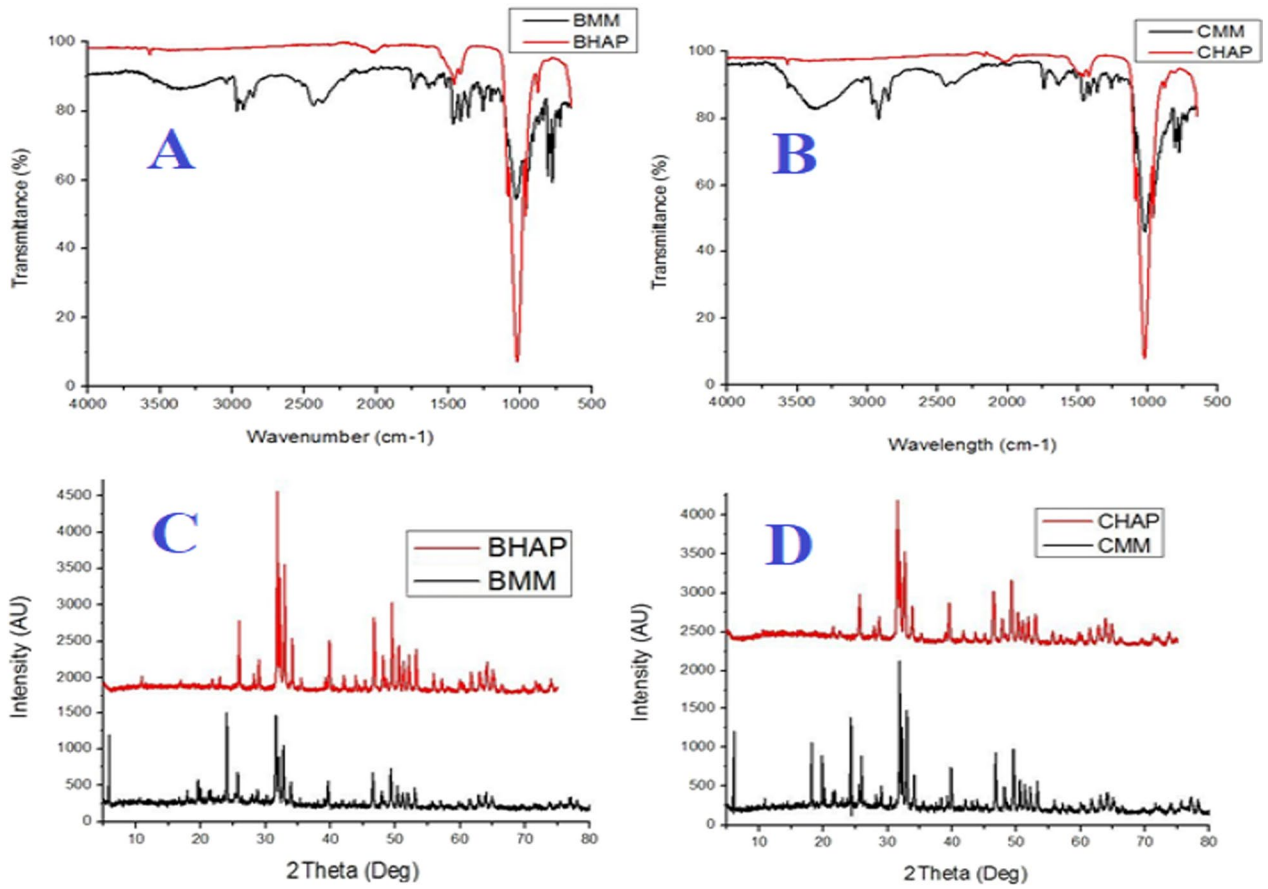

Fig. 2 FTIR Spectra of **A** BMM and BHAP, **B** CMM and CHAP; and XRD Patterns of **C** BMM and BHAP **D** CMM and CHAP

Table 4 Encapsulation efficiency and drug loading capacity of the HAP samples

Capped HAP codes	MUP concentration in ethanol (ug/ml)	MUP mass in 100 ml ethanol (g)	MUP encapsulated in HAP (g)	HAP encapsulation efficiency (%)	HAP drug loading capacity (mg/g)
BHAP	10,540	1.0540	2.9460	73.65	295
CHAP	11,373	1.1373	2.8627	71.57	286

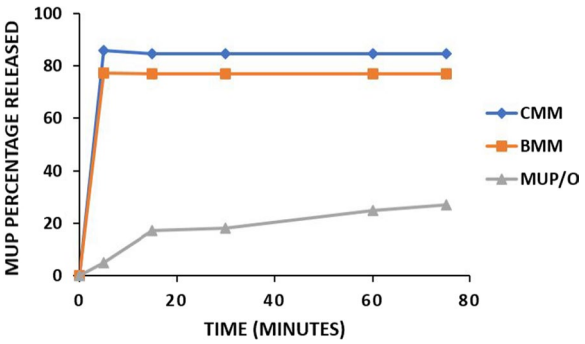

Fig. 3 Percentage of MUP Released from CMM, BMM and MUP/O

3.4.3 In-vivo and histological studies

The wounds images of the diabetic animals showing contraction as the treatment days elapsed and histological photomicrograph are shown pictorially (with different magnifications) in Fig. 7 from day 0 to day 16. Also, Fig. 6 shows that formulation CMM gave the highest wound closure area (377.8 mm^2) at day 16 of all the formulations used for the treatment. This was followed by BMM and BHAP with wound closure area of 357.2 and 295 mm^2, respectively. The control animals and the ones treated with MUP/O had the lowest wound closure area of 211.2 and 231.5 mm^2, respectively. The control animals had the lowest healing rate and HAP formulation (without API) showed a relatively better wound closure rate than the control animals.

The histological skin tissue samples were evaluated for histomorphometry with the results shown in Fig. 8.

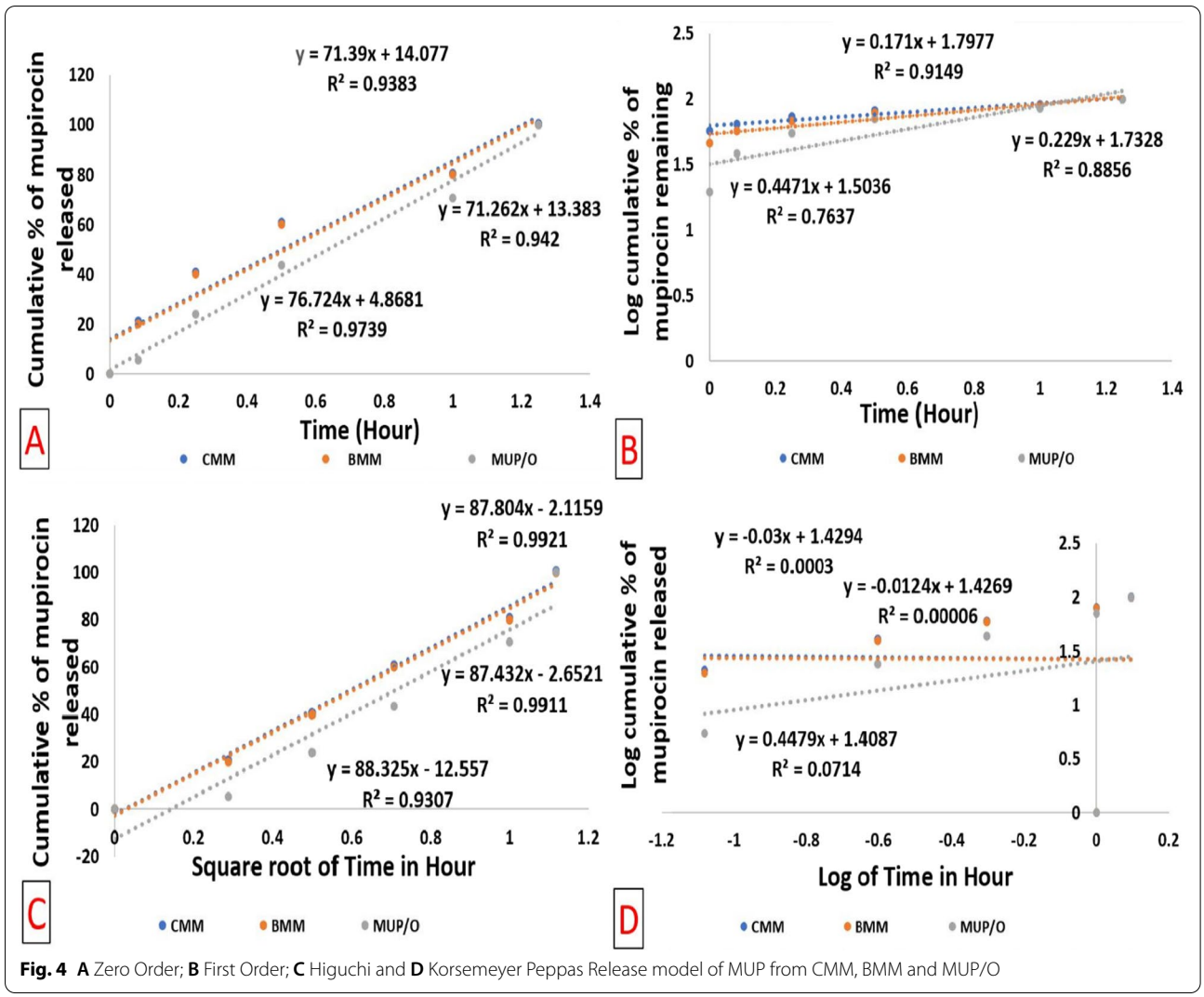

Fig. 4 **A** Zero Order; **B** First Order; **C** Higuchi and **D** Korsemeyer Peppas Release model of MUP from CMM, BMM and MUP/O

Table 5 Mathematical model for MUP release kinetic data

Formulation code	Zero order (R^2)	First order (R^2)	Higuchi (R^2)	Korsemeyes Peppas	
				(R^2)	(*n*) slope
CMM	0.9383	0.9149	0.9921	0.0003	− 0.03
BBM	0.942	0.8856	0.9911	0.00006	− 0.0124
MUP/O	0.9739	0.7637	0.9307	0.0714	0.4479

The tissue in control samples shows skin with underlying loose fibro-collagenous stroma (dermis) containing sebaceous glands and hair follicles. The stratum fibrosum was separated into bands by adipose tissue with highest level of inflammatory cells (950 cell/mm^2 of field). But for the ones treated with ordinary BHAP, it showed skin with underlying loose fibro-collagenous stroma (dermis), keratotic lesion on the epidermis, with several inflammatory cells admixed with increased granulation tissue significant with wound healing, distorted sebaceous glands and hair follicles were also seen, with the inflammatory cells (899 cell/mm^2 of field) deep into the subcutaneous fat layer. The diabetic animals treated with MUP/O, BMM and CMM formulations showed skin with underlying loose fibro-collagenous stroma (dermis) containing sebaceous glands and hair follicles. The stratum

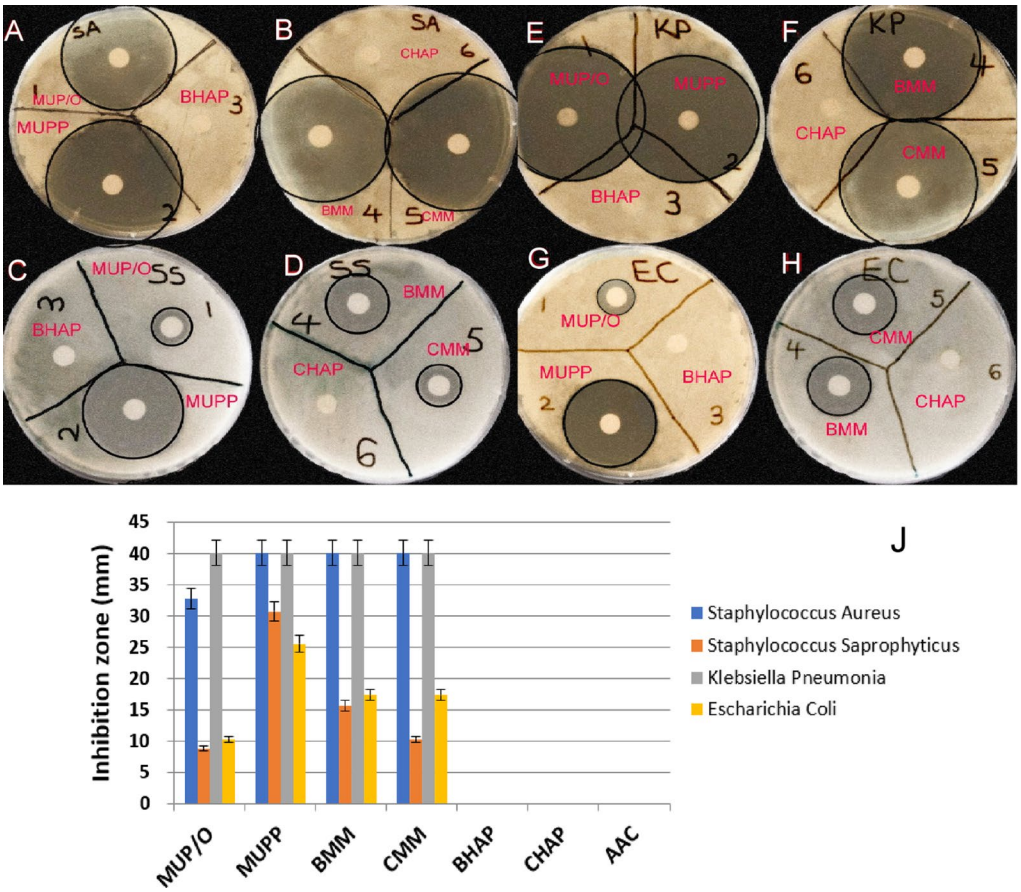

Fig. 5 **A**–**H** Microbial plates showing evaluation of antibacterial activity of the formulations against *Staphylococcus aureus (SA),* Staphylococcus *saprophyticus (SS), Klebsiella pneumonia (KP) and Escherichia coli (ES)* and **J** The graphical representation of inhibition of zones against the bacteria

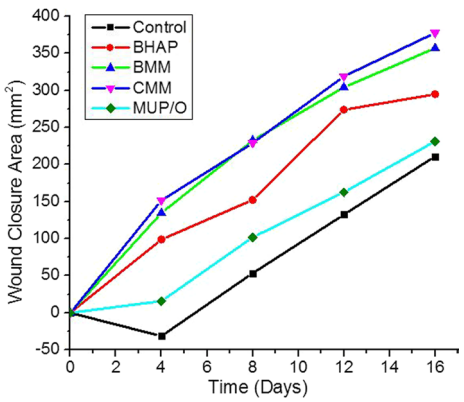

Fig. 6 Wound closure area with days in the animals treated with the formulations and control

fibrosum was separated into bands by adipose tissue; this also showed increased granulation tissue significant with wound healing and no abnormalities were seen. Thickness of the central region of the epidermis to the dermis was comparatively lower in BHAP and CMM. In BBM, the percentage occupied by collagen was 69%/mm^2 of field while that of control was 23%/mm^2 of field. The re-epithalization rate was 94.78% and 42.45% in BMM and BHAP samples, respectively. Also, BBM had the lowest number of inflammatory cell (189 cell/mm^2 of field) and shortest desquamated epithelial region (2.48 mm).

4 Discussion

These days, HAP has strongly positioned itself to be used clinically in form of powders, granules, dense and porous blocks, and with various composites, which could be attributed to its great biocompatibility and bioactivity properties [32, 33]. Though the HAP does not have any antimicrobial activity against any of the selected bacteria, it has been proven to be compatible with MUP in hydrogel to combat chronic wound. After the calcination process at 1000 °C, the percentage weight loss of the BBS and CBS was 37% and 45.4%, respectively. This represents the quantity of the organic component expelled from the bones which can be said to be more in CBS than in BBS.

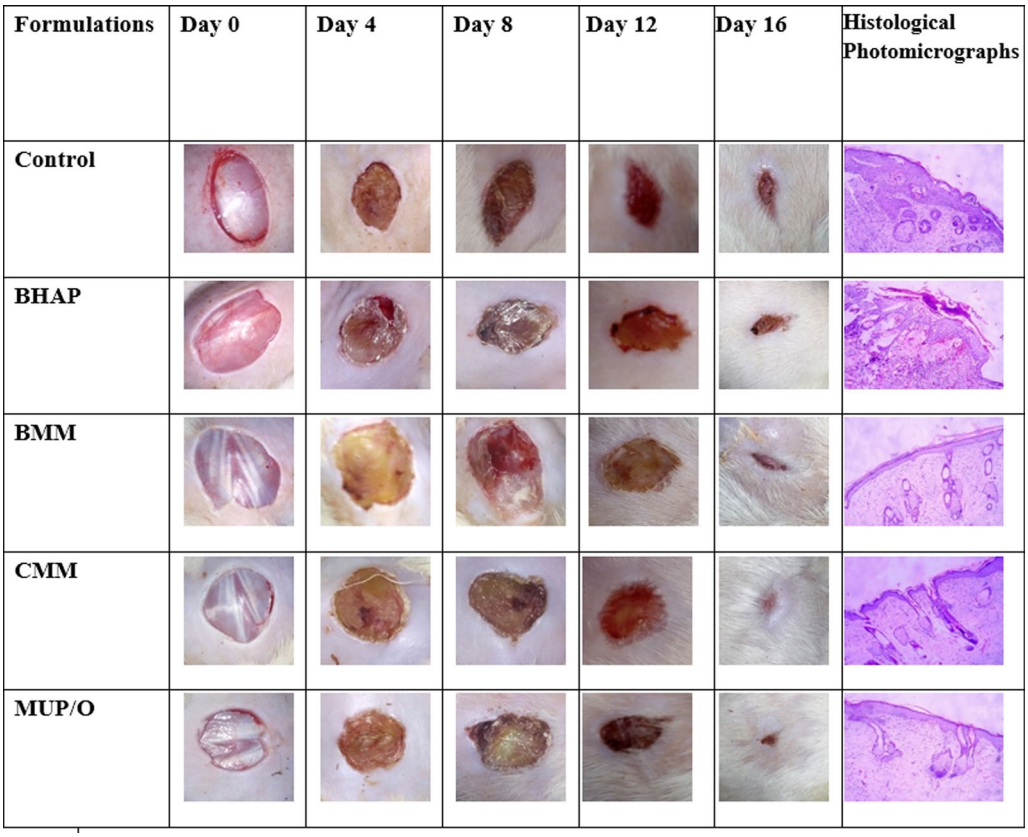

Fig. 7 Wounds images showing contraction as the treatment days elapsed and histological photomicrographs

The irregularity in size and shape of raw BBS and CBS morphology and low surface area after milling might be due to the presence of collagen binding the particles in the raw samples, which would make it tougher and subsequently more resistance to milling [22]. The superior surface area of calcined bone samples over the raw could be attributed to less energy requirement for their size reduction after the expulsion of the organic moiety during calcination. The oil yields after pressing the MOS two weeks after harvest were 3%, while it was 19.6% after twelve weeks. This difference in the yield was due to the fact that the seeds might have been denatured while keeping them and the protein in the seed solidified and denatured at elevated temperature, so that oil was separated from the protein [34]. Thus, roasting the seeds can increase the oil yield but may, however, decrease the quality and shelf life of the oil [35]. The seed storage time before extraction affects the oil yield of moringa seed as the yield increased with the number of weeks the seeds were kept. However, this relationship is not expected to be linear at all time. The XRD peaks at $2\theta = \sim 6$ and 24°, which correspond to that of MUP in BMM and CMM which did not appear BHAP and CHAP in the XRD patterns. These intense and sharp characteristic peaks in BBM and CMM XRD patterns indicate the active presence and crystalline nature of MUP in the samples. Similarly, the FTIR spectra showed MUP bands in BMM and CMM; this equally confirms that the MUP was still present in them after drug loading. The drug release study showed that the drug release rate was higher in hydrogels than in ointment (oil based). The relatively lower release of MUP from the ointment may be either as a result of the ointment base used in the formulation did not permit the drug to diffuse into the dissolution media or it could have high affinity toward the MUP drug molecule. The data obtained from the kinetic showed that the formulations CMM and BMM data fitted better to Higuchi kinetics having their R^2 greater than 0.99, while MUP/O followed zero-order kinetics. This is an indication that the drug release from the matrix of CMM and BMM was due to diffusion [36].

The MUP/O having low wound closure rate despite containing an API and showing antimicrobial activities against some selected bacterial. This could be attributed to low percentage drug release established during the drug release study. Its MUP was not encapsulated by any drug carrier to be able to efficiently tackle the

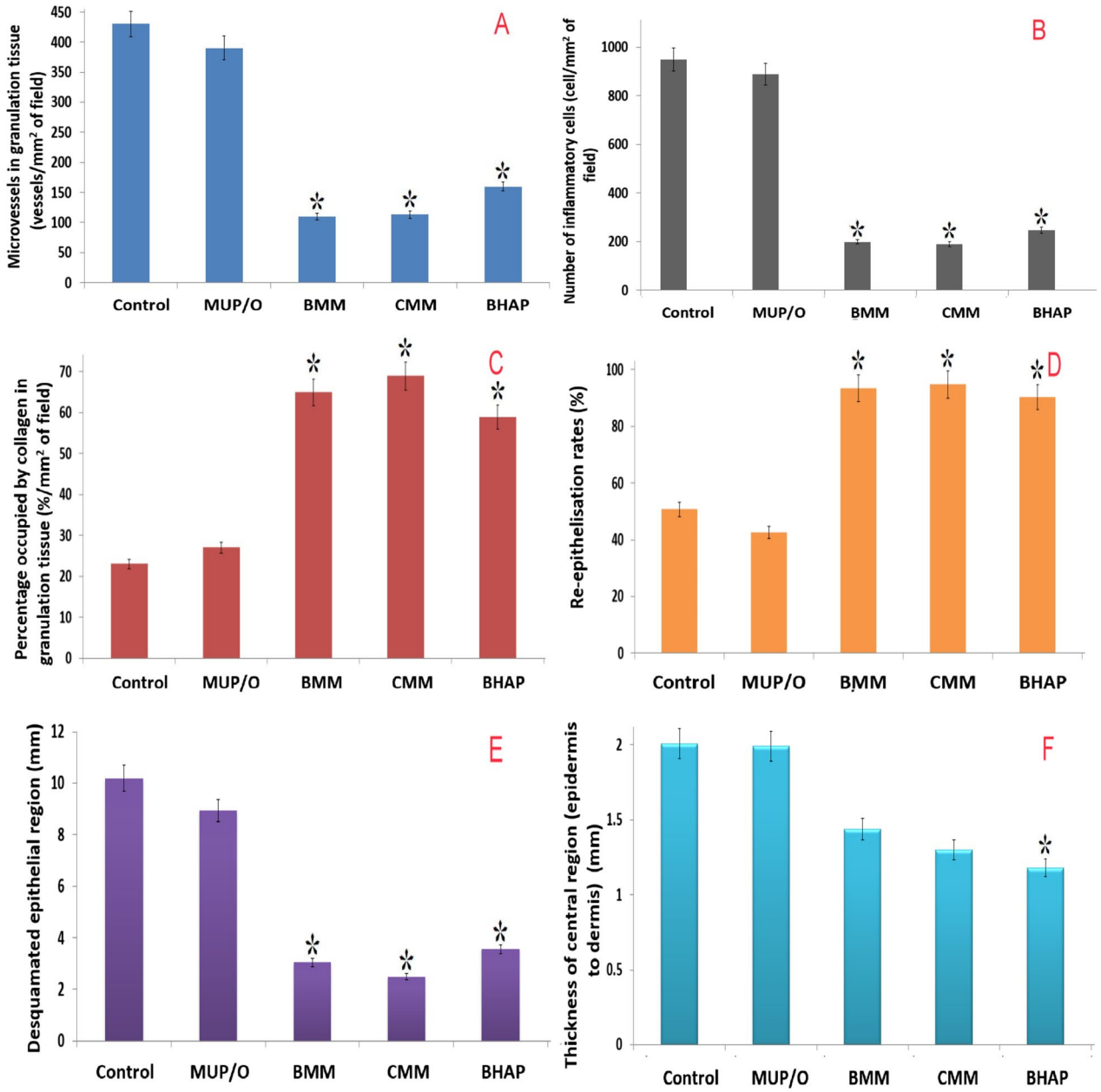

Fig. 8 Histomorphometry values showing: **A** Micro vessels in granulation tissues (vessels/mm^2 of field), **B** Numbers of inflammatory cells (cell/mm^2 of field), **C** Percentages of collagen occupied regions in granulation tissues in granulation tissues (% mm^2 of field) **D** Re-epithelization rate (%) **E** Desquamated epithelium regions (mm) and **F** Thicknesses of central regions of granulation tissues from epidermis to dermis (mm); *$p < 0.05$

advanced complexity of chronic wounds like excessive of proteases [18] and biofilms [15] formation. The BHAP formulation showed a relatively better wound closure rate than the control animals. This could be possibly because hydrogel promotes the epithelization and reconstruction of skin tissues on full thickness wound as revealed by Ilomuanya et al. [30]. Also, the hydrogel keeps the wounds moist and hydrated which enhances the re-epithelialization [37]. As expected, the control animals had the lowest wound closure area rate because no form of treatment except cleaning and dressing was done on their wounds. BHAP had the highest viscosity value (2602 ± 23 MPa) of all the prepared formulations as shown in Table 1. This may be due to the fact that it did not contain MUP like the

BMM and CMM. The addition of MUP might have led to the reduction in their viscosity.

The evaluation of microbial activities revealed that the MUPP had the overall highest inhibition zone against each of the four bacteria. This was possibly because the MUPP was neither encapsulated in any drug carrier nor contained in any gelling agents like hydrogel which tend to reduce the antimicrobial activity of the API slightly. Similarly, it was clear that the BHAP and CHAP did not have any antimicrobial activity against any of the bacteria used in this study and thus marginally reduced the dynamic of the MUP in the formulation. The same was applicable in case of MUP/O, which had the petroleum and mineral oil as its base composition. The healing activities of the formulations on the diabetic wound were examined more distinctively with histological analysis. The tissue in control samples having highest level of inflammatory cells (950 cell/mm^2 of field) was because nothing was applied on the wound resulting in uncontrolled multiplication of bacterial in the wound. Despite the accelerated wound closure rate of the ones treated with BHAP, which was more than that of MUP/O, Fig. 8b shows that the inflammatory cells in BHAP (889 cell/mm^2) were astronomically higher than that of MUP/O (199 cell/mm^2). This revealed that high wound closure rate should not be confused with proper wound healing. It is possible for a wound to experience the former without the latter and vice versa. It was only the BMM and CMM that were able to achieve the two simultaneously. The percentage occupied by collagen in granulation tissue and re-epithelialization rate were higher in formulations with MUP. They also showed lower thickness of the central region of the epidermis to the dermis. Their excellent results in histomorphometry parameters had made them to have significantly higher wound healing rate on the animals treated with the formulations than others as they contained encapsulated API necessary for chronic wound healing process. The proper analysis of the photomicrograph (X100) and histomorphometry data shown in Figs. 7 and 8, respectively, revealed that the animals treated with BMM seemed to have the best healing response and the control animals showed the worst.

5 Conclusions

This study explored the use of the HAP isolated from bovine and caprine bones to formulate encapsulated MUP-HAP hydrogel composite for management of chronic wound. The CMM had the highest encapsulation efficiency and drug loading capacity of 73.65% and 295 mg/g, respectively, and the highest drug release of 84.67% of MUP in 75 min, while the MUP/O released 27.04% after same time during in vitro drug release study. The CMM and BMM hydrogel formulations showed Higuchi kinetic release model, while the MUP/O showed zero order. Based on wound closure rate, the BMM and CMM proved to be 54.32% and 63.17% better than the conventional ointment (MUP/O) in the management of chronic wound. The in-vivo study and histomorphometry analysis revealed that the formulations prepared from MUP encapsulated in BHAP and CHAP were able to achieve high wound closure rate and proper wound healing unlike the MUP/O which was without HAP drug carrier.

Abbreviations

BBS: Bovine bone sample; CBS: Caprine bone sample; HAP: Hydroxyapatite; BHAP: Hydroxyapatite obtained from bovine bone; CHAP: Hydroxyapatite obtained from caprine bone; BMM: Capped bovine bone particles loaded with mupirocin; CMM: Capped caprine bone particles loaded with mupirocin; MUP: Mupirocin; MUP/O: Conventional Mupirocin ointment; API: Active pharmaceutical ingredient.

Acknowledgements

Not Applicable.

Author contributions

OEO contributed to execution of experimental design, collation of data, interpretation of results and manuscript writing. MOI, OIS, OPG, SOA contributed to conceptualization of design, monitoring of experiments, reading and correction of manuscript. All authors read and approved the final manuscript.

Funding

Not applicable.

Availability of data and materials

All data and material are available upon request.

Declarations

Ethics approval and consent to participate

Ethical approval was obtained from the Health Research and Ethics committee of the College of Medicine University of Lagos. All the experiments accorded with the Institution Guidelines and were approved by College of Medicine University of Lagos Health Research Ethical Committee (CMUL/HREC/03/21/829).

Consent for publication

Not applicable.

Competing interests

The authors declare nonexistence of competing interests.

Author details

[1]Department of Metallurgical and Materials Engineering, Faculty of Engineering, University of Lagos, Akoka, Lagos, Nigeria. [2]Projects Development and Design Department, Federal Institute of Industrial Research, Cappa Bus Stop, Oshodi, Lagos, Nigeria. [3]Department of Pharmaceutics and Pharmaceutical Technology, Faculty of Pharmacy, University of Lagos, Idi– Araba, Lagos, Nigeria. [4]Department of Industrial Engineering, Durban University of Technology, Durban, South Africa.

Received: 14 March 2022 Accepted: 3 June 2022
Published online: 18 June 2022

References

1. De-Jalon EG, Blanco-Prieto MJ, Ygartua P, Santoyo S (2001) Topical application of acyclovir-loaded microparticles: quantification of the drug in porcine skin layers. J Control Release 75:191–197
2. Mathur P, Jha S, Ramteke S, Jain NK (2018) Pharmaceutical aspects of silver NPs. Artif Cells Nanomed Biotechnol 46:115–126. https://doi.org/10.1080/21691401.2017.1414825
3. Heng BC, Zhao X, Xiong S, Ng KW, Boey FY, Loo JS (2010) Toxicity of zinc oxide (ZnO) nanoparticles on human bronchial epithelial cells (BEAS-2B) is accentuated by oxidative stress. Food Chem Toxicol 48:1762–1766
4. Bohner M, Tadier S, van Garderen N, de Gasparo A, Döbelin N, Baroud G (2013) Synthesis of spherical calcium phosphate particles for dental and orthopedic applications. Biomatter. https://doi.org/10.4161/biomatter.25103
5. Pokhrel S (2018) Hydroxyapatite: preparation, properties and its biomedical applications. Adv Chem Eng Sci 8:225–240. https://doi.org/10.4236/aces.2018.84016
6. Kantharia N, Naik S, Apte S, Kheur M, Kheur S, Kale B (2014) Nano-hydroxyapatite and its contemporary applications. JDRSD 1:15–19
7. Mohammed AMH (2015) Synthesis of hydroxyapatite nanoparticles. pp 70
8. Szczes A, Holysz L, Chibowski E (2017) Synthesis of hydroxyapatite for biomedical applications. Adv Coll Interface Sci 249:321–330
9. Hashemi SA, Madani SA, Abediankenari S (2015) The review on properties of aloe vera in healing of cutaneous wounds. Biomed Res Int 2015:714216
10. Bodeker G, Hughes A (1998) Wound healing, traditional treatments and research policy plants for food and medicine. Royal Botanic Garden, London, pp 245–359
11. Wilkinson HN, Hardman MJ (2020) Wound healing: cellular mechanisms and pathological outcomes, wound treatment and skin regeneration. J Nanobiotechnol. https://doi.org/10.1098/rsob.200223
12. Whitney JA (2005) Overview: acute and chronic wounds. Nurs Clin North Am 40:191–205
13. Ilomuanya MO, Adebona AC, Wang W, Sowemimo A, Eziegbo CL, Silva BO, Adeosun SO, Joubert E, De Beer D (2020) Development and characterization of collagen based electrospun scafolds containing silver sulphadiazine and aspalathus linearis extract for potential wound healing applications. Springer Nat Appl Sci 2:881. https://doi.org/10.1007/s42452-020-2701-8
14. Kelso M (2021) The importance of acidic pH on wound healing: why all the (pH)uss about microenvironments? Woundsource Blog.www.woundsource.com.
15. Kim M (2016) Nanoparticle-based therapies for wound biofilm infection: opportunities and challenges. Nanobioscience 15(3):294–304. https://doi.org/10.1109/TNB.2016.2527600
16. Edwards JV, Howley P, Cohen IK (2004) In vitro inhibition of human neutrophil elastase byoleic acid albumin formulations from derivatized cotton wound dressings. Int J Pharm 284(1–2):1–12
17. Schönfelder U, Abel M, Wiegand C, Klemm D, Elsner P, Hipler UC (2005) Influence of selected wound dressings on PMN elastase in chronic wound fluid and their antioxidative potential in vitro. Biomaterials 26(33):6664–6673
18. Krishnaswamy VR, Manikandan M, Munirajan AK, Vijayaraghavan D, Korrapati PS (2014) Expression and integrity of dermatopontin in chronic cutaneous wounds: a crucial factor in impaired wound healing. Cell Tissue Res 358(3):833–841. https://doi.org/10.1007/s00441-014-2000-z. PMID25260909.S2CID16355532
19. Losi P, Briganti E, Magera A, Spiller D, Ristori C, Battolla B, Balderi M, Kull S, Balbarini A, Di SR (2010) Tissue response to poly(ether)urethane-polydimethylsiloxane-fibrin composite scaffolds for controlled delivery of proangiogenic growth factors. Biomaterials 31:5336–5344
20. Amrutiya N, Bajaj A, Madan M (2009) Development of microsponges for topical delivery of mupirocin. AAPS PharmSciTech 10(2):402. https://doi.org/10.1208/s12249-009-9220-7
21. Putnam CD, Reynolds MS (1989) Mupirocin: a new topical therapy for impetigo. J Pediatr Health Care 3(4):224–227
22. Ojo OE, Sekunowo OI, Ilomuanya MO, Gbenebora OP, Adeosun SO (2022) Structural and morphological evaluations of natural hydroxyapatite from calcined animal bones for biomedical applications. J Cast Mater Eng 6(1):14–21. https://doi.org/10.7494/jcme.2022.6.1.14
23. Abdalla KF, Kamoun EA, El Maghraby GM (2015) Optimization of the entrapment efficiency and release of ambroxol hydrochloride alginate beads. J Appl Pharm Sci 5(04):13–019. https://doi.org/10.7324/JAPS.2015.50403
24. Ilomuanya MO, Okafor PS, Amajuoyi JN, Onyejekwe JC, Okubanjo OO, Adeosun SO, Silva BO (2020) Polylactic acid-based electrospun fiber and hyaluronic acid-valsartan hydrogel scaffold for chronic wound healing. Beni-Suef Univ J Basic Appl Sci 9:31. https://doi.org/10.1186/s43088-020-00057-9
25. Dash S, Narasimha PM, Nath I, Chowdhury P (2010) Kinetic modeling on drug release from controlled drug delivery systems. Acta Poloniae Pharm Drug Res 67(3):217–223
26. Baratam SR, Dhanalakshmi S (2018) Design and evaluation of zolpidem tartrate matrix tablets for extended release using natural gums and HPMC K100M. J Appl Pharm Sci 8(07):072–077. https://doi.org/10.7324/JAPS.2018.8712
27. Romes NB, Wahab RA, Hamid MA, Oyewusi HA, Huda N, Kobun R (2021) Thermodynamic stability, in-vitro permeability, and in-silico molecular modeling of the optimal *Elaeis guineensis* leaves extract water-in-oil nanoemulsion. Sci Rep. https://doi.org/10.1038/s41598-021-00409-0
28. Bereksi MS, Hassaïne H, Bekhechi C, Abdelouahid DE (2018) Evaluation of antibacterial activity of some medicinal plants extracts commonly used in algerian traditional medicine against some pathogenic bacteria. Pharmacogn J 10(3):507–512
29. Amajuoyi JN, Ilomuanya MO, Asantewaa-Osei Y, Azubuike CP, Adeosun SO, Igwilo CI (2020) Development of electrospun keratin/coenzyme Q10/poly vinyl alcohol nanofibrous scaffold containing mupirocin as potential dressing for infected wounds. Future J Pharm Sci 6:25. https://doi.org/10.1186/s43094-020-00043-z
30. Ilomuanya MO, Seriki A, Ubani-ukoma N, Oseni A, Silva BO (2020) Silver sulphadiazine- xanthan gum- hyaluronic acid composite hydrogel for wound healing: formulation development and in vivo evaluation. Nig J Pharm 16(1):21–29
31. Leone A, Spada A, Battezzati A, Schiraldi A, Aristil J, Bertoli S (2016) Moringa oleifera seeds and oil: characteristics and uses for human health. Int J Mol Sci 17:2141. https://doi.org/10.3390/ijms17122141
32. Ferraz MP, Monteiro FJ, Manuel CM (2004) Hydroxyapatite nanoparticles: a review of preparation methodologies. J Appl Biomat Biomecha 2:74–80
33. Kannan S, Rocha JH, Ventura JM, Lemos AF, Ferreira JM (2005) Effect of Ca/P ratio of precursors on the formation of different calcium apatitic ceramics—an X-ray diffraction study. Scr Mater 53:1259–1262
34. Seedoilpress (2021) Oilseeds roasting, good way to increase oil yield. Retrieved June 17, 2021 from roasting oilseeds help you largely increase the oil yield (seedoilpress.com)
35. Tulashie SK, Kotoka F, Appiah AP, Awuah P, Baiden KA (2018) Effects of roasting and boiling on the yield quality and oxidative stability of extracted soya bean oil. Therm Sci Eng. https://doi.org/10.24294/tse.v1i2.424
36. Maru SM, Gathu LW, Mathenge AW, Okaru AO, Kamau FN, Chepkwony HK (2012) In vitro drug release studies of metronidazole topical formulations through cellulose membrane. East Cent Afr J Pharm Sci 15:57–62
37. Ousey K, Cutting KF, Rogers AA, Rippon MG (2016) The importance of hydration in wound healing: reinvigorating the clinical perspective. J Wound Care 25(3):122–130. https://doi.org/10.12968/jowc.2016.25.3.122

Publisher's Note

Springer Nature remains neutral with regard to jurisdictional claims in published maps and institutional affiliations.